

Magnetotransmission of microwaves through potassium slabs

Graciela Lacueva

Department of Physics, John Carroll University, University Heights, Ohio 44118

A. W. Overhauser

Department of Physics, Purdue University, West Lafayette, Indiana 47907

(Received 3 May 1993)

Five signals which emerge after transmission through potassium slabs (~ 0.1 mm thick) have been studied by Dunifer, Sambles, and Mace at 1.3 K with 79-GHz microwaves and large magnetic fields, $H\hat{z}$, perpendicular to the slabs. They are (i) conduction-electron-spin resonance (together with spin-wave sidebands); (ii) Gantmakher-Kaner (GK) oscillations; (iii) cyclotron resonance; (iv) cyclotron-resonance subharmonics; and (v) high-frequency oscillations. Spin-resonance transmission has been understood for many years, but not the other four. The isotropic-Fermi-surface model is used here to calculate the transmitted power versus H by solving Maxwell's equations self-consistently with the Boltzmann transport equation. GK oscillations do emerge, but the (theoretical) transmitted power is too large by a factor ~ 10000 . In contrast, the remaining three signals should not even exist. It has been shown that a charge-density-wave broken symmetry creates a family of (higher-order) minigaps which cuts through the Fermi surface near its extremities along the slab normal. These gaps diminish the effectiveness of conduction electrons having v_z near the Fermi velocity. Calculation confirms that this ineffectiveness dramatically reduces the predicted amplitude of the GK oscillation, and thereby provides an interpretation of the huge discrepancy. The minigaps also give rise to a small Fermi-surface cylinder which (as recently shown) leads to Landau-level oscillations that quantitatively explain signal (v). Signals (iii) and (iv) can also be attributed to the small Fermi-surface cylinder, but only because its axis is tilted $\sim 45^\circ$ relative to \hat{z} . A nonlocal theory for such a scenario is yet to be formulated.

I. INTRODUCTION

From a theoretical point of view, potassium is a most important metal. Being monovalent and having Brillouin-zone energy gaps of only ~ 0.4 eV, its Fermi surface is thought (by some) to be spherical to $\sim 0.1\%$. Lithium could have been the exemplar, except that below ~ 78 K it undergoes a martensitic phase transformation (from bcc) to a rhombohedral structure having a nine-layer stacking sequence.¹ This phase change destroys cubic symmetry and thereby precludes a simple characterization of low-temperature electronic behavior. The Fermi surface is no longer simply connected. A similar situation exists for sodium below ~ 35 K.² In contrast, potas-

sium retains its bcc structure to 4 K, as is known from neutron diffraction³ and ultrasonic attenuation⁴ on strain-free crystals. Accordingly, potassium plays the dominant role in the confrontation between theory (for a simple metal) and reality.

The focus of this work is on the transmission of microwaves through potassium slabs in a magnetic field, $H\hat{z}$, perpendicular to the sample. An extensive study of the five signals that emerge is due to Dunifer, Sambles, and Mace,⁵ who reported data on 15 potassium samples. Four of the transmission signals for sample K-4 (kindly provided to us by G. L. Dunifer) are shown versus ω_c/ω in Fig. 1. $\omega_c \equiv eH/m^*c$, and $m^* = 1.21 m$.⁶ Not shown

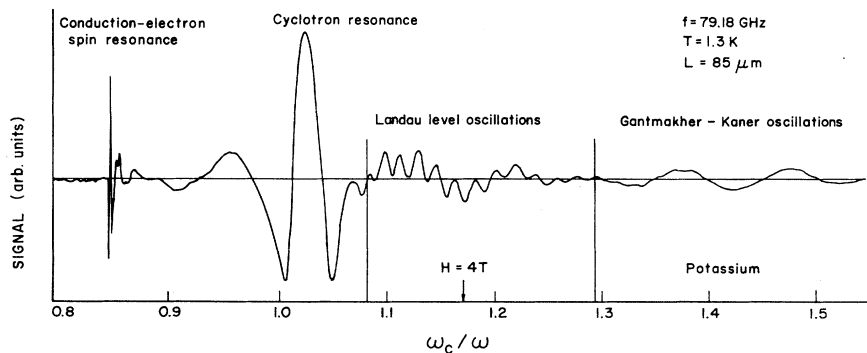


FIG. 1. Microwave transmission signal vs H through a potassium slab in a perpendicular magnetic field. ($H = 3.42$ T at $\omega_c/\omega = 1$). The phase of the microwave reference was adjusted so that the cyclotron resonance is symmetric. The data are from sample K-4 of Ref. 5. Not shown is the signal between $\omega_c/\omega = 0$ and 0.8, which exhibits cyclotron-resonance subharmonics at $\frac{1}{2}$, $\frac{1}{3}$, and $\frac{1}{4}$. The Gantmakher-Kaner oscillations in the low-field range are smaller than those near $\omega_c/\omega = 1.5$ by a factor of 5.

are the subharmonic cyclotron resonances at $\omega_c/\omega = \frac{1}{2}$, $\frac{1}{3}$, and $\frac{1}{4}$. ($\omega/2\pi$ is the microwave frequency f .) Sample K-4, 85 μm thick, was selected by G. L. Dunifer for the overall clarity of its transmission signals. The amplitude of its Gantmakher-Kaner (GK) signal was consistent with those from other samples, whether formed in argon or in vacuum.

Conduction-electron-spin-resonance transmission, and the associated spin-wave sidebands, have been studied extensively⁷ and provide the only phenomenon of the five which is correctly accounted for by a simple theoretical model. (Even in this case, however, sideband splittings indicate⁸ the presence of a charge-density-wave broken symmetry.⁹) Unlike the spin precession signal, which is collective in nature, the four remaining signals are critically dependent on the one-electron energy spectrum and the Fermi-surface topology. Magnetotransmission of microwaves is therefore an important tool for validating or contradicting theoretical points of view.

To gain perspective it is useful to display the field dependence of the transmission signal when the electrical conductivity is local. That is, the current density (in the $\hat{x}\hat{y}$ plane) can be obtained from¹⁰

$$\mathbf{j}(z) = \frac{\sigma_0}{1 + (\omega_c\tau)^2} \begin{pmatrix} 1 & -\omega_c\tau & 0 \\ \omega_c\tau & 1 & 0 \\ 0 & 0 & 1 + (\omega_c\tau)^2 \end{pmatrix} \mathbf{E}(z), \quad (1)$$

where \mathbf{j} and \mathbf{E} are column vectors, and $\sigma_0 = ne^2\tau/m^*$ (τ being the relaxation time, and n the electron density). The sample configuration is here a semi-infinite specimen, and $H\hat{z}$ is normal to the surface. The (transverse) electric field at $z=0$ is

$$\mathbf{E} = E_0 \hat{x} e^{-i\omega t}. \quad (2)$$

On using Maxwell's curl equations, together with Eq. (1), one finds two propagating microwave fields:

$$E_{\pm} = (E_x \pm iE_y) = E_0 e^{i(q_{\pm}z - \omega t)}, \quad (3)$$

where

$$q_{\pm} = \left[\frac{4\pi\omega i\sigma_0/c^2}{1 - i(\omega \pm \omega_c)\tau} \right]^{1/2}. \quad (4)$$

Figure 2 shows the field dependence of the two circularly polarized microwave signals at a depth $d = 2 \times 10^{-6}$ cm. The field variable is represented by ω_c/ω , for $f = 79.18$ GHz. ($\omega_c/\omega = 1$ when $H = 3.42$ T.) The relaxation time τ was chosen so that $\omega_c\tau = 70$, which causes a cyclotron-resonance width equal to that of the resonance in Fig. 1.

Notice that the E_+ wave increases monotonically with increasing H . In contrast, the E_- wave exhibits a sharp cyclotron-resonance dip at $\omega_c/\omega = 1$. The sharp dip at resonance is the only important transmitted feature. The reason for the dip can be understood from Eq. (4). At resonance the microwave skin depth for the E_- mode, $1/\text{Im}(q_-)$, reaches its minimum value. Off resonance, the denominator in Eq. (4) becomes large, and so the skin

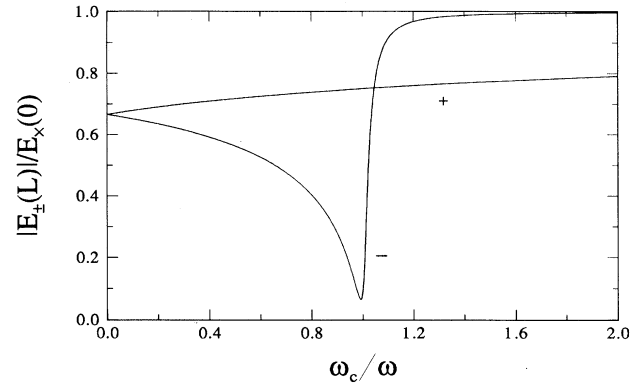


FIG. 2. Field dependence of the circularly polarized microwave signals at a depth $d = 2 \times 10^{-6}$ cm if the conductivity σ_0 is local, i.e., for propagation constants given in Eq. (4). The sharp dip near $\omega_c/\omega = 1$ occurs in the wave which rotates with the same sense as an electron's cyclotron motion. ($\omega_c\tau = 70$.)

depth increases, indicating a greater penetration of the microwave field.

Needless to say, the local conductivity Eq. (1) does not apply to potassium at 1.3 K. The conduction-electron mean free path $l = v_F\tau$ is then much larger than the skin depth. Accordingly a nonlocal theory must be used to determine the transmitted signal. Nevertheless, the most significant intuition that can be gained from Fig. 2 is that a standard theoretical model leads to a cyclotron-resonance dip in the transmitted power. This expected behavior is contradicted by the very large resonance peak in the data of Fig. 1. Such a peak occurs in all samples.⁵

Before proceeding to the nonlocal theory, it is necessary to define the transmission efficiency in absolute terms. Consider a slab (of thickness L) which is infinite in the $\hat{x}\hat{y}$ plane. Suppose the incident microwave field (on the surface at $z=0$) has an energy flux P_0 (in ergs/cm² s). Because the reflection coefficient is almost unity, the electric fields of the incident and reflected waves at $z=0$ will almost cancel. However, the magnetic fields will add. For a linearly polarized incident wave, $E'_x = H'_y$. The reflected wave (at $z=0$) will have $E''_x \cong -E'_x$ and $H''_y \equiv H'_y$. So the total fields at the front surface are $E_x \cong 0$ and $H_y \cong 2H'_y$.

At the rear surface ($z=L$), there is only an outgoing wave. If only the \hat{x} polarized component were detected, the transmitted field (at $z=L$) will have $E_x(L) \cong H_y(L)$. The ratio of the transmitted power P_t to P_0 is, therefore,

$$\frac{P_t}{P_0} \cong \left| \frac{E_x(L)}{\frac{1}{2}H_y(0)} \right|^2. \quad (5)$$

This definition is general; it applies to the local-conductivity calculation, based on Eq. (4), as well as to the nonlocal ones which will follow below.

For the (theoretical) local case treated above, with $\tau = 1.4 \times 10^{-10}$ s, $f = 79.18$ GHz, and $n = 1.4 \times 10^{22}$ cm⁻³, the classical skin depth in the low-field limit is $\approx |q|^{-1}$, which from Eq. (4) is

$$\delta_0 = 5 \times 10^{-6} \text{ cm}. \quad (6)$$

It is necessary to include both e^{iqz} and e^{-iqz} waves in order to match continuity equations for \mathbf{E} and \mathbf{H} at both surfaces. Then the power transmission ratio, from (5), (6), and Maxwell's curl \mathbf{E} equation, is, for $L = 85 \mu\text{m}$,

$$\frac{P_t}{P_0} \cong \left[\frac{8\pi f \delta_0}{c} \exp(-L/\delta_0) \right]^2 \sim 10^{-1500}, \quad (7)$$

which is rather small. Nonlocal effects are necessary to explain the existence of a transmitted signal.

II. NONLOCAL THEORY FOR AN ISOTROPIC FERMI SURFACE

The conduction-electron mean free path $l = v_F \tau$ in potassium (of typical purity) below 4 K is ~ 0.1 mm, i.e., ~ 100 times the (nonlocal) skin depth for microwaves. The transverse conductivity can be found by solving self-consistently the Boltzmann transport equation together with Maxwell's equations. This exercise is a well-known one, so we shall merely quote the result for $\sigma_{\pm}(q, \omega, H)$ that we derived for a related problem:¹¹

$$\sigma_{\pm} = \frac{3ne^2\tau}{2m^*x^2} \{ 2ap - 1 + r(x^2 + 1 - a^2) + i[a + p(x^2 + 1 - a^2) - 2ar] \}, \quad (8)$$

where

$$\begin{aligned} a &= (\omega \pm \omega_c) \tau, \\ x &= ql, \\ p &= \frac{1}{4x} \ln \left[\frac{1 + (x+a)^2}{1 + (x-a)^2} \right], \\ r &= \frac{1}{2x} [\tan^{-1}(x+a) + \tan^{-1}(x-a)]. \end{aligned} \quad (9)$$

Application of this result to transmission of microwaves through a slab of thickness, L , is facilitated when one assumes that the two surfaces are smooth, so that specular reflection of electrons occurs. Sensitive experiments¹² involving potassium that has crystallized in contact with glass have shown that specularly is readily achieved.

Following the formalism of Urquhart and Cochran,¹³ we expand the field and current distributions (for $0 < z < L$) in a Fourier cosine series:

$$E_{\pm}(z) = \sum_{n=0}^{\infty} E_{\pm}^n \cos(q_n z), \quad (10)$$

$$j_{\pm}(z) = \sum_{n=0}^{\infty} \sigma_{\pm} E_{\pm}^n \cos(q_n z), \quad (11)$$

where $q_n = n\pi/L$. From Maxwell's curl equations it follows that

$$\frac{\partial^2 E_{\pm}}{\partial z^2} = -\frac{4\pi i \omega}{c^2} j_{\pm}. \quad (12)$$

(This displacement-current term has been dropped.) The coefficients E_{\pm}^n can be obtained by using (11) and (12) and multiplying the resulting equation by $\cos(q_m z)$, followed

by an integration from 0 to L . One finds, with E'_{\pm} denoting $\partial E_{\pm}/\partial z$,

$$E_{\pm}^m = \frac{(2 - \delta_{m0})[(-1)^m E'_{\pm}(L) - E'_{\pm}(0)]}{L[q_m^2 - (4\pi i \omega/c^2)\sigma_{\pm}(q_m)]}, \quad (13)$$

where δ_{m0} is 1 for $m=0$, and zero otherwise. The integral involving the left-hand side of (12) must be carried out by partial integration, without using (10). The reason for this caution is that the series for E'_{\pm} converges to 0 at $z=0$ and L , whereas (in fact) E'_{\pm} is finite at both surfaces.

Suppose, for the time being, that the sample were very thick. Then a solution of interest is a propagating wave in the \hat{z} direction. $E'_{\pm}(L)$ can be set to zero in Eq. (13). $E'_{\pm}(0)$ may be evaluated from Maxwell's curl \mathbf{E} equation, which requires

$$E'_{\pm} = \pm \frac{\omega}{c} H_{\pm}(0). \quad (14)$$

If the incident electromagnetic wave (for $z < 0$) is polarized along \hat{x} , then $\mathbf{H}(0)$ is along \hat{y} . We now take the total $H_y(0)$, from incident and reflected waves, to be 1 cgs unit, so that

$$H_{\pm}(0) = \pm i. \quad (15)$$

Accordingly, the right-hand side of Eq. (14) is $i\omega/c$. The coefficients (13) for the \hat{z} -propagating solution are then

$$E_{\pm}^m = -i \frac{\omega}{cL} (2 - \delta_{m0}) [q_m^2 - (4\pi i \omega/c^2)\sigma_{\pm}(q_m)]^{-1}. \quad (16)$$

At the rear surface $z=L$, there will arise a reflected wave traveling along $-\hat{z}$. The two waves at $z=L$ must combine so that $|H|$ and $|E|$ are equal, because that is required by the boundary conditions appropriate to having only a transmitted wave (for $z > L$). Inside the metal, $|H|$ for a traveling wave is several orders of magnitude larger than $|E|$. Accordingly, the two waves must combine so that (at $z=L$) the magnetic fields almost cancel. The opposite Poynting vectors then require that the two contributions to \mathbf{E} are essentially equal and parallel. Recognizing this factor of 2, the electric field at $z=L$ is

$$E_{\pm}(L) = -i \frac{2\omega}{cL} \sum_{m=0}^{\infty} \frac{(2 - \delta_{m0}) \cos(m\pi)}{q_m^2 - (4\pi i \omega/c^2)\sigma_{\pm}(q_m)}. \quad (17)$$

A detailed analysis which leads to this factor of 2 has been presented by Cochran.¹⁴ From Eq. (5) and $H_y(0) \equiv 1$, the transmitted power ratio for a detector sensitive to polarization π is

$$P_{\pi}/P_0 = 4|E_{\pi}(L)|^2. \quad (18)$$

It will be shown below that for the sample of Fig. 1, the observed ratio is $\sim 10^{-22}$, i.e., 220 decibels below the power incident on the metal surface from the microwave configuration.

Evaluation of Eq. (17) presents numerical difficulty because the series converges very slowly and, moreover, is an alternating one, since $\cos(m\pi) = (-1)^m$. Nevertheless, a successful calculation results from following the method of Ref. 13. The first 3000 terms can be summed without compromise. For $m > 3000$, one can replace the

denominator of Eq. (16) by q_m^2 . Accordingly, one must calculate

$$\sum_{3001}^{\infty} \frac{(-1)^m}{m^2} = \sum_1^{\infty} \frac{(-1)^m}{m^2} - \sum_1^{3000} \frac{(-1)^m}{m^2} \quad (19)$$

(precision to 14 decimals is required.) The first term on the right-hand side is $-\pi^2/12$, and the second causes no numerical problem. We have verified that the results to be presented below are unaltered when the cutoff is changed from 3000 to 5000.

Figure 3 shows the *predicted* amplitude of $E_+(L)$ and $E_-(L)$ for the conditions of Fig. 1. Observe that the cyclotron resonance is a *moderate* and *broad dip* in E_0 near $\omega_c/\omega=1$. Both waves exhibit oscillations having half the GK period. Figure 4 shows the transmitted signal $E_{\hat{x}}(L)$. Observe the prominent (GK) oscillations, but notice that near $\omega_c/\omega=1$ there is only a small decrease in the oscillation amplitude. There is no evidence of a sharp cyclotron resonance peak, there are no cyclotron resonance subharmonics, and there are no high-frequency oscillations between $\omega_c/\omega=1.1$ and 1.3, as in Fig. 1.

The periodicity of the GK oscillation is related to the Fermi velocity v_F of the conduction electrons, and depends on the sample thickness L . The phenomenon is caused by those electrons having the fastest velocity parallel to \mathbf{H} . Each oscillation occurs when the number of cyclotron rotations during the transit time, L/v_F , is an integer n , i.e.,

$$n = \omega_c L / 2\pi v_F. \quad (20)$$

On setting $\omega_c = eH_n/m^*c$ and $v_F = \hbar k_F/m^*$, Eq. (20) leads to GK peaks H_n which are linear in n :

$$H_n = (2\pi\hbar k_F/eL)n. \quad (21)$$

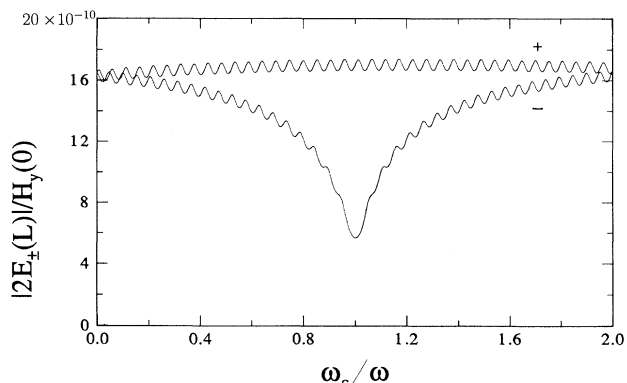


FIG. 3. Theoretical field dependence of the circularly polarized microwave-transmission amplitudes for a potassium slab of thickness $L = 85 \mu\text{m}$. The broad, symmetric dip at $\omega_c/\omega=1$ occurs in the signal rotating with the cyclotron motion. The nonlocal conductivity Eq. (8) for an isotropic Fermi surface was employed. ($\omega_c\tau=70$.) The periodicity of the oscillations is half that of Gantmakher-Kaner oscillations (which do not occur in the circularly polarized amplitudes). The small oscillations correspond to ballistic transit times for electrons, having $|v_z|=v_F$, and which travel from $z=0$ to L and back again, being an integral multiple of the cyclotron period.

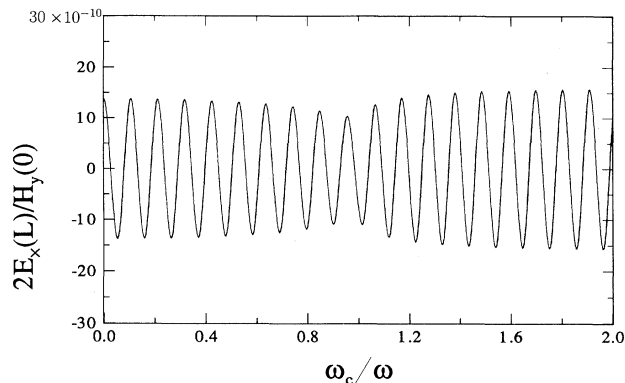


FIG. 4. Theoretical field dependence of the linearly polarized microwave-transmission amplitude for a potassium slab of thickness $L = 85 \mu\text{m}$. The nonlocal conductivity Eq. (8) for an isotropic Fermi surface was employed. There is no cyclotron resonance peak and, of course, no Landau-level oscillations. The power transmission ratio is the square of the ordinate, $2E_x(L)/H_y(0)$, and exceeds that observed in the Gantmakher-Kaner oscillations of Fig. 1 by 2×10^4 .

Notice that m^* cancels out, so the oscillation period provides a measure of the Fermi-surface radius k_F .

The foregoing characteristics of the GK signal were verified in many specimens.⁵ However, what has never been tested until now, to our knowledge, is the absolute magnitude of the GK signal. Equation (18) together with the amplitude of $E_{\hat{x}}(L)$ near $\omega_c/\omega=1.5$ in Fig. 4 leads to a *theoretical* power transfer ratio at the maximum in the oscillation,

$$P_t/P_0 = 2 \times 10^{-18}. \quad (22)$$

G. L. Dunifer has kindly provided the calibration of his microwave-transmission instrument. The power transfer ratio was $3s^2 \times 10^{-23}$, where s is the detector output in μv . From the original chart recordings of Fig. 1, $s \approx 2\mu\text{v}$ near $\omega_c/\omega=1.47$. Accordingly, the *experimental* power transfer ratio is

$$P_t/P_0 \approx 1 \times 10^{-22}. \quad (23)$$

The discrepancy between (22) and (23)—a factor exceeding 10000—is serious. It cannot be attributed to sample imperfection, e.g., rough or nonparallel surfaces. Such causes would degrade the GK resonances for high values of H_n compared to low ones. Such is not the case. The GK oscillation near $\omega_c/\omega \sim 1.5$, i.e., $H = 5.1 \text{ T}$, which corresponds to $n \sim 14$ in Eq. (21), is considerably larger than those for $n = 1-5$ (not shown in Fig. 1). Dunifer, Sambles, and Mace⁵ report that larger GK signals for $\omega_c/\omega > 1$ are usually observed. Furthermore, spin-wave sidebands, which are also geometric resonances, are routinely observed out to $n = 30-50$.⁷ Consequently, geometric imperfection of samples cannot be imputed. We have also verified that the prediction (22), for which $\omega_c\tau=70$ was used, is not sensitive to variations in τ by factors of 2. In Sec. III we shall show that altered Fermi-surface topology created by a charge-density-wave

broken symmetry can account for the extreme weakness of the observed GK signal.

III. SUPPRESSION OF GK OSCILLATIONS BY A CHARGE-DENSITY WAVE

The existence of a charge-density-wave (CDW) broken symmetry¹⁶ in potassium has been established by many extraordinary electronic properties,^{9,17} that now number ~ 30 . The wave vector \mathbf{Q} of the CDW is tilted about 1° away from a [110] crystal direction; so in a large crystal 24 \mathbf{Q} domains are possible. The theory of the 1° tilt¹⁸ stems from the elastic anisotropy of potassium. Phonon screening of the CDW requires less elastic stress if $\mathbf{Q}^* = \mathbf{G}_{110} - \mathbf{Q}$, i.e., the wave vector of the three phonon modes involved, is tilted about 45° from the [110] axis closest to \mathbf{Q} .

An important property of potassium is that when thin specimens crystallize in contact with smooth, amorphous silica or sapphire, the (polycrystalline) grains are epitaxially oriented. Each grain (usually) has a [110] direction perpendicular to the surface. (The reason is that {110} planes are the most closely packed.) The CDW charge modulation of the conduction electrons can optimize the interfacial energy if the direction of \mathbf{Q} is also close to the surface normal. This behavior is indicated, for example, by the anisotropic optical conductivity,^{9,19} and has also been noticed with low-energy electron diffraction.

The conduction-electron energy spectrum is profoundly affected by the CDW periodic potential $G \cos(\mathbf{Q} \cdot \mathbf{r})$. In addition to the energy gaps defined by \mathbf{Q} , there are two families of higher-order gaps which arise when the crystal potential $V \cos(\mathbf{G}_{110} \cdot \mathbf{r})$, is also in the Schrödinger equation.²⁰ The "heterodyne" gaps are described by the Fourier components

$$\mathbf{Q}_n = n(\mathbf{G}_{110} - \mathbf{Q}) = n\mathbf{Q}^*, \quad (24)$$

and the "minigaps" correspond to

$$\mathbf{Q}_m = (m + 1)\mathbf{Q} - m\mathbf{G}_{110} \quad (25)$$

(m and n are integers). Some of the predicted infrared transitions²¹ made possible by these gaps have been reported experimentally.²² The Fermi-surface topology which takes into account the tilt of \mathbf{Q} and \mathbf{Q}^* relative to the [110] axis has been elaborated.²³ A schematic view of the (001) plane in the Brillouin zone is shown in Fig. 5. For clarity we have exaggerated the disparity between $|\mathbf{Q}|$ and $|\mathbf{G}_{110}|$, which is actually only 1.5%. (The figures in Ref. 23 are accurate.)

The horizontal direction in Fig. 5 is the magnetic-field direction \hat{z} in the transmission experiments. It is self-evident that fast electrons traveling in the \hat{z} direction will have their cyclotron rotation interrupted by the minigaps. Consequently their contribution to the GK signal will cease. A possible way to model this effect is to let the scattering time τ be a continuous function of v_z . (Any artificial discontinuity will introduce spurious oscillations in the signal.) A simple option is to replace τ , which we redefine as τ_0 , by

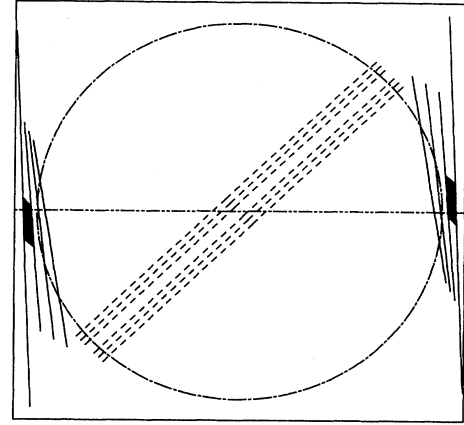


FIG. 5. The $k_z=0$ plane of the Brillouin zone of potassium. The horizontal axis is along [110] and is parallel to \mathbf{H} . The three sets of (dashed) energy-gap planes passing near the center are heterodyne gaps, having periodicities defined by Eq. (24). The three sets of (solid and short) energy-gap planes near the extremities (along \mathbf{H}) are minigaps having periodicities defined by Eq. (25). The pair of planes nearest the zone boundary are the main CDW energy gaps. The two black volumes, when joined end to end, describe a Fermi-surface cylinder, having an axis tilted $\sim 45^\circ$ from [110]. The cylinder's volume is $\sim 4 \times 10^{-4}$ times that of the (undistorted) Fermi sphere, which is also shown.

$$\tau = \frac{\tau_0}{1 + y|v_z/v_F|}, \quad (26)$$

so that scattering times become short for electrons having v_z near the minigap regions (y is an adjustable parameter). $\sigma_{\pm}(q, \omega, H)$ must be reevaluated, starting from Eq. (13) of Ref. 11 (but with τ inside the integral). Instead of Eq. (8),

$$\sigma_{\pm} = \frac{3ne^2\tau_0}{4m^*} \left\{ \frac{2(y^2 - x^2)}{(y^2 + x^2)^2} - \frac{y}{y^2 + x^2} + f_1 p_1 - g_1 r_1 + f_2 p_2 - g_2 r_2 + i \left[f_1 r_1 + g_1 p_1 + f_2 r_2 + g_2 p_2 - \frac{2a(y^2 - x^2)}{(y^2 + x^2)^2} \right] \right\}. \quad (27)$$

$x = ql$ and $a = (\omega \pm \omega_c)\tau$, as in Sec. II, and

$$f_1 = [(1 - a^2 - y^2 + x^2)(3yx^2 - y^3) + 2(a + yx)(3y^2x - x^3)] / (x^2 + y^2)^3, \\ g_1 = [2(a + yx)(y^3 - 3yx^2) + (1 - a^2 - y^2 + x^2)(3y^2x - x^3)] / (x^2 + y^2)^3, \quad (28)$$

$$p_1 = \frac{1}{2} \ln \left[\frac{(a - x)^2 + (y + 1)^2}{(1 + a^2)} \right],$$

$$r_1 = \tan^{-1} \left[\frac{ay + x}{y + 1 + a^2 - xa} \right].$$

Furthermore, $f_2(x)=f_1(-x)$, $g_2(x)=g_1(-x)$, $p_2(x)=p_1(-x)$, and $r_2(x)=r_1(-x)$.

The transmission signal for $y=6$ was computed as described above, and is shown in Fig. 6. As expected, the GK oscillations are substantially reduced, and can be as small as desired by increasing y . The summation break [see Eq. (19)] had to be extended to 10 000.

The problem that remains is why, if Fig. 5 is correct, there are any GK signals at all. Cyclotron rotation of electrons having $v_z \approx v_F$ is thwarted by the minigaps. The answer is that even though most CDW domains will have \mathbf{Q} perpendicular to the sample face, there can be a few domains for which \mathbf{Q} is $\sim 60^\circ$ from the [110] surface normal (near another [110] direction). One may surmise from Fig. 5 that, in this event, "clear" regions of the Fermi surface can occur along the axis parallel to \mathbf{H} .

The sizes of the minigaps and heterodyne gaps fall off very quickly^{20,23} with the integers n and m in (24) and (25). Consequently, many of the gaps will lose their effectiveness as a result of magnetic breakdown—a high-field phenomenon. Possibly the larger GK signals (seen at high fields) can be explained by magnetic breakdown of the weaker minigaps and heterodyne gaps which would, in small fields, jeopardize the cyclotron motion of electrons responsible for the GK periodicity.

The physical presence of minigaps and heterodyne gaps has been decisively confirmed by the extensive open-orbit resonance experiments of Coulter and Datars,²⁴ phenomena that are accounted for quantitatively with a CDW structure.²⁵ There seems to be little risk in concluding that the discrepant (10 000-fold) loss in GK signal has a similar origin.

IV. CONCLUSION

The foregoing treatment brings into comprehension one more of the five microwave signals that emerge from potassium. Only two remain to be explained, since the high-frequency oscillations were recently shown to be Landau-level oscillations belonging to a small Fermi-surface cylinder formed by the minigaps.²⁶ This cylinder, which is pieced together from the two black cylinders shown in Fig. 5, contains only 4×10^{-4} electrons per atom.¹¹ This small number was sufficient, however, to explain the sharp cyclotron resonance peak in the microwave surface impedance.²⁷ The cross-sectional area ($\pi k_F^2/69$) of the cylinder, determined from the Landau-level periodicity (vs $1/H$),²⁶ when combined with the cylinder length (determined from CDW neutron-diffraction satellites²⁸), agrees with the originally surmised fraction 4×10^{-4} . Landau-level oscillations from the main Fermi surface, having a cross section πk_F^2 , are too rapid and too small to be seen in a microwave transmission experiment. (They have been studied frequently by the de Haas–van Alphen effect.)

Adding a cylindrical Fermi-surface component to the microwave transmission theory does not (with the cylinder axis parallel to \hat{z}) explain the cyclotron reso-

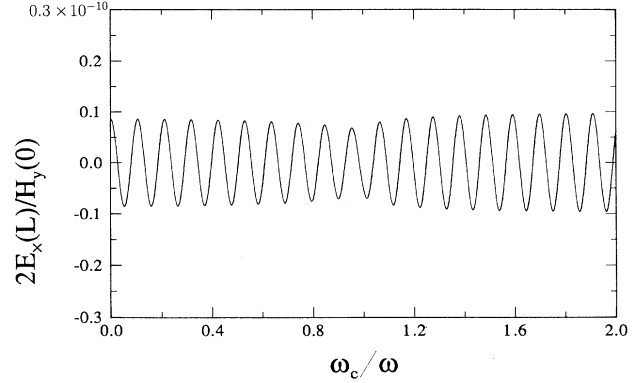


FIG. 6. Theoretical field dependence of the Gantmakher-Kaner transmission signal based on the nonlocal conductivity Eq. (27), having a v_z -dependent scattering time given by Eq. (26) with $y=6$. The power transmission ratio is the square of the ordinate, and equals the value 1×10^{-22} , observed near $\omega_c/\omega=1.5$ in Fig. 1. Magnetic breakdown of minigaps and heterodyne gaps can be simulated by letting y be a decreasing function of H . Accordingly, the GK amplitude would then increase with H , as is observed.

nance peak (near $\omega_c/\omega=1$), even if the modified σ_{\pm} , Eq. (27), is employed. We believe that the 45° tilt of the cylinder axis that is required theoretically^{18,23} plays a crucial role. This tilt is the only possible explanation for the cyclotron-resonance subharmonics because, then, the individual orbits (in real space) oscillate back and forth along \hat{z} (as well as rotate in the $\hat{x}\hat{y}$ plane). Such back and forth motion along the electric field gradient is the behavior which creates subharmonics in the Azbel-Kaner effect.²⁹

A nonlocal theory which incorporates a cylindrical Fermi surface tilted $\sim 45^\circ$ relative to \mathbf{H} presents a formidable theoretical endeavor. The reduced symmetry destroys the isolation of the E_+ and E_- fields, and the longitudinal oscillations of the cylinder orbits introduce coupling to plasma modes. A quantitative explanation of the dominant microwave-transmission signal—the large and ubiquitous cyclotron resonance peak—will likely remain pending until a nonlocal study can be brought to completion.

ACKNOWLEDGMENTS

We are especially indebted to Professor G. L. Dunifer for sending us the original recorder traces of his microwave transmission data for sample K-4, for developing the absolute calibration of his instruments, and for his advice in helping us to quantify the power transmission ratio reliably. We are grateful to Mi-Ae Park for independently verifying the calculations. Professor J. F. Cochran kindly pointed out the expansion technique for treating transmission through slabs of finite thickness. Finally, we are indebted to the National Science Foundation for financial support.

- ¹A. W. Overhauser, *Phys. Rev. Lett.* **53**, 64 (1984).
- ²R. Berliner, O. Fajen, H. G. Smith, and R. L. Hitterman, *Phys. Rev. B* **40**, 12 086 (1989).
- ³S. A. Werner, A. W. Overhauser, and T. M. Giebultowicz, *Phys. Rev. B* **41**, 12 536 (1990).
- ⁴David Kubinski and J. Trivisonno, *Phys. Rev. B* **47**, 1069 (1993).
- ⁵G. L. Dunifer, J. F. Sambles, and D. A. H. Mace, *J. Phys. Condens. Matter* **1**, 875 (1989).
- ⁶C. C. Grimes and A. F. Kip, *Phys. Rev.* **132**, 1991 (1963).
- ⁷D. A. H. Mace, G. L. Dunifer, and J. F. Sambles, *J. Phys. F* **14**, 2105 (1984).
- ⁸Yong Gyoo Hwang and A. W. Overhauser, *Phys. Rev. B* **38**, 9011 (1988); see especially Figs. 7, 8, and 9.
- ⁹A. W. Overhauser, *Adv. Phys.* **27**, 343 (1978).
- ¹⁰Charles Kittel, *Introduction to Solid State Physics*, 6th ed. (Wiley, New York, 1986), p. 155.
- ¹¹G. Lacueva and A. W. Overhauser, *Phys. Rev. B* **33**, 3765 (1986).
- ¹²P. A. Penz and T. Kushida, *Phys. Rev.* **176**, 804 (1968).
- ¹³K. B. Urquhart and J. F. Cochran, *Can. J. Phys.* **64**, 796 (1986).
- ¹⁴J. F. Cochran, *Can. J. Phys.* **48**, 370 (1970).
- ¹⁵Murray R. Spiegel, *Mathematical Handbook of Formulas and Tables* (McGraw-Hill, New York, 1968), formula 19.22, p. 108.
- ¹⁶A. W. Overhauser, *Phys. Rev.* **167**, 691 (1968).
- ¹⁷A. W. Overhauser, in *Highlights of Condensed-Matter Theory, Proceedings of the International School of Physics "Enrico Fermi," Course LXXXIX, Varenna on Lake Como, 1983*, edited by F. Bassini, F. Fumi, and M. P. Tosi (North-Holland, Amsterdam, 1985), p. 194.
- ¹⁸G. F. Giuliani and A. W. Overhauser, *Phys. Rev. B* **20**, 1328 (1979).
- ¹⁹A. W. Overhauser and N. R. Butler, *Phys. Rev. B* **14**, 3371 (1976).
- ²⁰F. E. Fragachan and A. W. Overhauser, *Phys. Rev. B* **29**, 2912 (1984).
- ²¹F. E. Fragachan and A. W. Overhauser, *Phys. Rev. B* **31**, 4802 (1985).
- ²²Yu M. Kobzar' and B. N. Bodnar, *Pis'ma Zh. Eksp. Teor. Fiz.* **52**, 686 (1990) [*JETP Lett.* **52**, 37 (1990)].
- ²³Yong Gyoo Hwang and A. W. Overhauser, *Phys. Rev. B* **39**, 3037 (1989).
- ²⁴P. G. Coulter and W. R. Datars, *Can. J. Phys.* **63**, 159 (1985).
- ²⁵M. Huberman and A. W. Overhauser, *Phys. Rev. B* **25**, 2211 (1982).
- ²⁶Graciela Lacueva and A. W. Overhauser, *Phys. Rev. B* **46**, 1273 (1992). Equation (17) of this paper is missing a factor ω in the numerator.
- ²⁷G. A. Baraff, C. C. Grimes, and P. M. Platzman, *Phys. Rev. Lett.* **22**, 590 (1969).
- ²⁸T. M. Giebultowicz, A. W. Overhauser, and S. A. Werner, *Phys. Rev. Lett.* **56**, 2228 (1986).
- ²⁹C. Kittel, *Quantum Theory of Solids* (Wiley, New York, 1963), p. 315.